

Research Report 23

JANUARY 1957

Tensile Strength Properties of Ice adhering to Stainless Steel



**SNOW, ICE AND PERMAFROST
RESEARCH ESTABLISHMENT**
Corps of Engineers, U. S. Army

Research Report 23

JANUARY 1957

Tensile Strength Properties of Ice adhering to Stainless Steel

by H. H. G. Jellinek

SNOW ICE AND PERMAFROST RESEARCH ESTABLISHMENT

Corps of Engineers, U. S. Army

Wilmette, Illinois

PREFACE

This work was carried out by Dr. Jellinek, physical chemist, under a personal service contract with the Corps of Engineers at the SIPRE laboratories, under the general direction of Mr. J. A. Bender, Acting Chief, Snow and Ice Basic Research Branch. This paper constitutes a progress report on SIPRE Project 22.1-31, Adhesive properties of ice.

It is the author's pleasure to thank Messrs. J. A. Bender, T. R. Butkovich, and Drs. A. Assur and J. K. Landauer for helpful discussions; Messrs. B. L. Hansen and L. E. Stanley for advice in the construction of the apparatus; and Dr. H. Bader for his interest in this work. The author is also indebted to Mr. G. M. Walker for valuable help in the execution of a large number of the experiments.

Manuscript received 10 October 1956

Department of the Army Project 8-66-02-004

CONTENTS

	Page
Preface -----	ii
Summary -----	iv
Introduction -----	1
Experimental -----	1
Materials -----	1
Preparation and mounting of specimens -----	1
Tensile strength apparatus -----	2
Experimental results -----	3
Tensile strength as a function of rate of loading -----	3
Tensile strength as a function of geometrical parameters -----	6
Temperature dependence -----	13
Discussion -----	13
Tensile strength as a function of rate of loading for snow ice -----	13
Tensile strength of ice cylinders as a function of geometrical parameters -----	14
References -----	22

ILLUSTRATIONS

Figures	Page
1. Mounting apparatus for larger ice cylinders -----	2
2. Horizontal mounting apparatus for thin disks of ice -----	3
3. Tensile strength apparatus -----	3
4. Typical breaks of snow-ice -----	3
5. Average tensile strength as a function of rate of stress appli- cation for snow-ice cylinders. (height 2 cm, diameter 2 cm)--	4
6. Typical rough surface of an ice film of original thickness 1.0×10^{-1} cm -----	7
7. Average tensile strength as a function of ice volume -----	7
8. Logarithms of average tensile strengths as a function of logarithms of the volumes -----	8
9. Logarithms of variances as a function of logarithms of volumes -----	8
10. Tensile strength as a function of cross-sectional area at constant volume -----	12
11. Log S-C/A versus logarithms of ice volume -----	12
12. Logarithms of tensile strengths as a function of the ratio H/D of height to diameter of the ice cylinder -----	14
13. Tensile strength as a function of cross-sectional area at constant height -----	21

TABLES

Table	Page
I. Tensile strength (kg/cm^2) of snow-ice cylinders adhering to stainless steel, as a function of rate of stress application----	4
II. Rates of loading and stress application as a function of rpm of motor for snow-ice -----	5
III. Rates of loading and stress application as a function of area and height of the specimens -----	5
IV. Tensile strength (kg/cm^2) for different cross-sectional areas and rates of stress application -----	6
V. Tensile strength (kg/cm^2) as a function of geometrical parameters, snow-ice cylinders adhering to stainless steel --	9
VI. Tensile strength (kg/cm^2) as a function of geometrical parameters, ice cylinders adhering to stainless steel -----	9

Table	Page
VII. Tensile strength (kg/cm ²) as a function of geometrical parameters, ice cylinders adhering to stainless steel -----	10
VIII. Tensile strength (kg/cm ²) as a function of geometrical parameters, ice cylinders adhering to stainless steel -----	10
IX. Tensile strength (kg/cm ²) as a function of geometrical parameters, ice cylinders adhering to stainless steel -----	11
X. Tensile strength (kg/cm ²) as a function of temperature, ice cylinders adhering to stainless steel -----	13

SUMMARY

Tensile strength measurements on ice cylinders adhering to stainless steel have been made as a function of rate of loading, thickness and cross-sectional area of specimens, and temperature. A rapid increase of tensile strength occurs as the volume is decreased and the data for a temperature of -4.5C can be represented over a thousandfold range of volumes by an equation as follows:

$$S = 2.74AV^{-0.84} + 9.4 \text{ kg/cm}^2$$

where \underline{S} is the tensile strength, \underline{A} the cross-sectional area in cm² and \underline{V} the volume in cm³. The experimental results are interpreted by means of a statistical treatment involving imperfections in the specimens. The statistics for a model consisting of a large number of parallel elements is elaborated. The final equation derived on statistical grounds approximates the equation found empirically, and reads as follows:

$$\bar{S}_{r,n} = kA^{1/\beta}V^{-1/\beta} + C$$

where $\bar{S}_{r,n}$ is the number average of the tensile strength, \underline{k} , $\underline{\beta}$, and \underline{C} are constants and r is the number of imperfections in each of \underline{n} parallel elements.

The conclusion reached is that the tensile strength is a statistical function of the volume and cross-sectional area of the specimens due to imperfections. Superimposed on to the statistical effect is a stress distribution effect, which becomes predominant for large volumes.

TENSILE STRENGTH PROPERTIES OF ICE ADHERING TO STAINLESS STEEL

by
H. H. G. Jellinek

INTRODUCTION

The tensile strength of solids as a function of their geometrical parameters presents interesting problems. The parts played by purely statistical effects on the one hand and stress distribution on the other do not yet appear to have been satisfactorily established. In this work ice cylinders have been investigated as a function of their cross-sectional area and height. The effect of rate of stress application to the specimens and the temperature dependence of tensile strength have also been studied.

There are numerous data on the bulk tensile strength of ice (see Butkovich, 1954, and references cited therein). However, tensile strength as a function of geometrical parameters has not yet been extensively investigated. The only works available are the reports on the chemical-physical nature of adhesion of ice to solid surfaces from the University of Cincinnati (Applied Science Research Laboratory, 1950-52; 1952-54; Berghausen *et al.*, 1953; 1955). These workers investigated the tensile strength properties of ice films sandwiched between carbon steel plugs at -25C. A sharp increase of strength with decreasing ice volume was noted. However, their experimental data show a rather large scatter so that a detailed evaluation is not possible. The data described in this work make such an analysis possible. It appears that the tensile strength of thin ice disks is dependent not only on their volume, but also on such geometrical parameters as cross-sectional area and height of the specimens.

An increase of strength with decreasing thickness is a general phenomenon, which has particularly been noticed in studies of adhesives (De Bruyne, 1951). The experimental data are discussed here in terms of theories based on statistical considerations, postulating distributions of imperfections in the ice, and on stress distributions in the specimens (Meissner and Baldauf, 1951). Papers concerning the statistics of probability distributions relevant to the present work have been published by Peirce (1926), Weibull (1939a, b), Daniels (1945), and Epstein (1948). In this paper, the statistics of imperfections, particularly of elements arranged in parallel, which were discussed to some extent in the papers mentioned above, is enlarged and elaborated.

EXPERIMENTAL

Materials

The larger ice cylinders (0.5 cm high and above) were prepared from snow-ice, which was obtained by sieving snow into water and subsequent freezing. The snow-ice used came from the same batch as that used in a previous investigation (Jellinek and Brill, 1956). Thin disks of ice, sandwiched between stainless steel cylinders, were prepared by freezing water which was freed of electrolytes by passing through exchange resin. Air was removed by boiling. Benzene was of Analar grade.

Preparation and mounting of specimens

To prepare the larger cylinders, a cube of snow-ice was frozen onto the roughened base of an aluminum cylinder. An ice cylinder of desired dimensions was then turned on a lathe at -10C. The aluminum cylinder plus the ice was placed into a mounting apparatus (Fig. 1), consisting essentially of a stainless steel frame with a stainless steel rod which can be moved vertically up and down, sliding in a ball bushing.

2 TENSILE STRENGTH PROPERTIES OF ICE ADHERING TO STAINLESS STEEL

The steel rod was exactly centered above an arrangement into which the aluminum cylinder was inserted. A stainless steel cylinder was attached to the bottom of the steel rod and heated to slightly above 0C by a heating wire wound around the lower end of the steel rod. The temperature of the steel cylinder was measured by a thermocouple and controlled by a Variac. Then the electric current was turned off and the steel cylinder was lowered and frozen to the snow-ice, forming only a small amount of water in the process. The aluminum cylinder was then cut off from the ice and the specimen turned over so that the stainless steel cylinder was in the position previously occupied by the aluminum cylinder. The process was repeated with a second stainless steel cylinder. The stainless steel was grade 304/A, with polished surface; the finishing polish used was Lapping Compound No. 38-900A, U.S. Products Company. The steel cylinders were kept in benzene, and were thoroughly cleaned with benzene before each experiment.

The thin cylinders or disks were prepared in a somewhat different way, using a modification of the previous mounting apparatus (Fig. 2). In this case, the apparatus is horizontal and the stainless steel rod is operated by turning a screw.

A Starrett gage was rigidly connected to the steel rod, which allowed distances to be measured within 2.5×10^{-4} cm. Two stainless steel cylinders were mounted in the apparatus and adjusted to the desired distance. Water was then introduced between the gap and seeded with ice, so that freezing took place within a few seconds. Any extraneous ice formed from waterdrops was carefully removed, either by a scalpel or on the lathe.

The mountings in either apparatus were carried out at -10C. Ten to fifteen minutes were allowed for each newly frozen interface before proceeding with the operation.

Tensile strength apparatus

The apparatus (Fig. 3) consists of a stainless steel frame and a threaded steel rod, which can be moved only vertically, driven by a three-phase motor through a worm gear and gear wheel. The loading speed can be varied by inserting different gear wheels in the motor. One revolution of the shaft leading from the motor to the apparatus corresponds to a vertical movement of about 3×10^{-3} cm. A Baldwin SR-4, U-1 500-lb cell was rigidly fixed to the lower end of the threaded steel rod. The ice specimen with its steel cylinders was hung onto the load cell by means of a flexible ball chain; and was hooked to the base of the steel frame by a similar chain.

The output of the Baldwin cell was recorded on a Leeds and Northrup recorder as a load versus time curve. The cell showed a linear relationship between output and load as specified by the manufacturer.

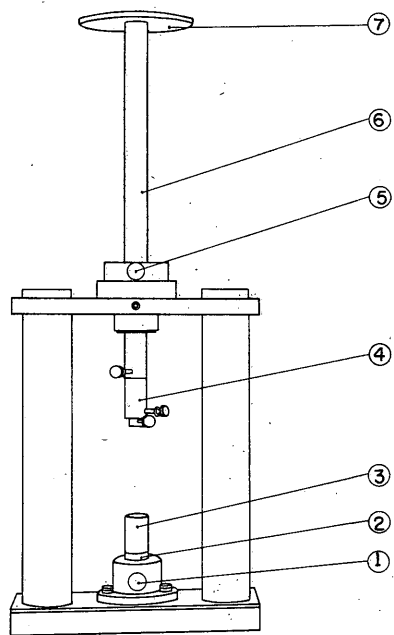


Figure 1. Mounting apparatus for larger ice cylinders (1) Set screw; (2) Stainless steel disk; (3) Ice specimen; (4) Adaptors; (5) Set screw; (6) Stainless steel rod; (7) Platform for weights.

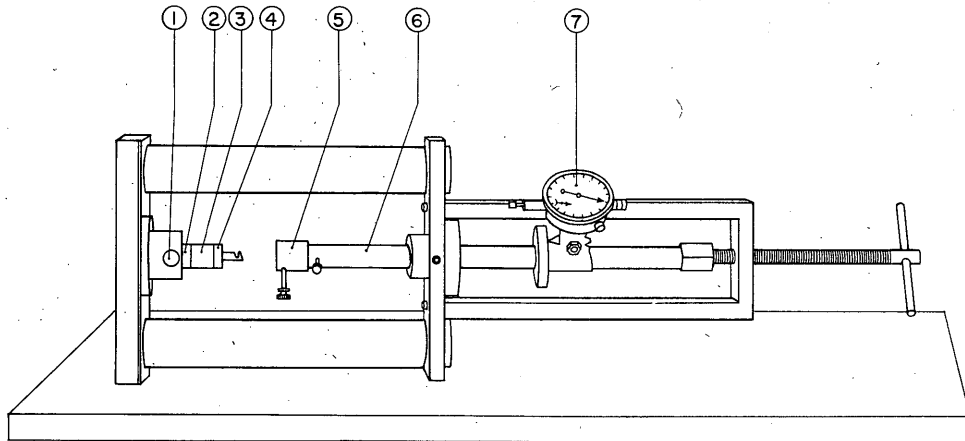


Figure 2. Horizontal mounting apparatus for thin disks of ice. (1) Set screw; (2) and (4) Stainless steel disks; (3) Ice specimen, (5) Adaptor; (6) Stainless steel rod; (7) Starrett gage.

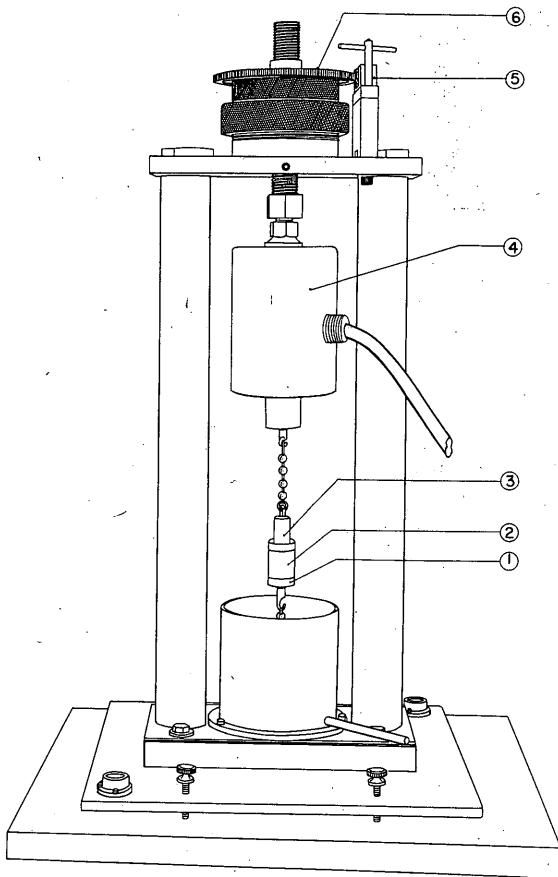


Figure 3. Tensile strength apparatus. (1) and (3) Stainless steel disks, (2) Ice cylinder, 2 cm high; (4) Baldwin load cell, SR-4, U-1, 500-lb, (5) Worm gear, (6) Gear wheel.

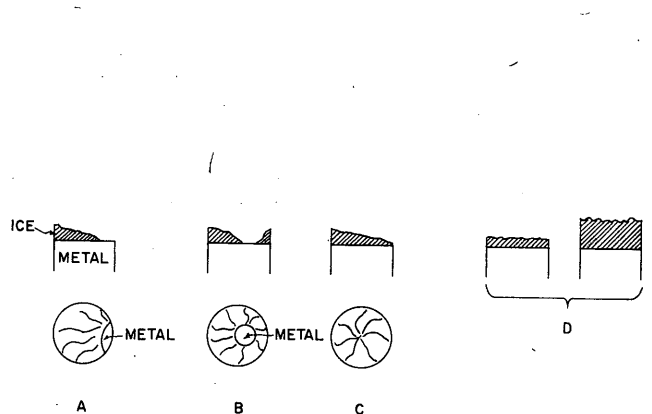


Figure 4. Typical breaks of snow-ice. (A,B) most frequent, (C) occasional, more frequent at high rates of loading, (D) Rare.

EXPERIMENTAL RESULTS

Tensile strength as a function of rate of loading

Cylinders of snow-ice of 2 cm height and 2 cm diam were tested at different rates of stress application. In most cases, twelve tests were carried out at each rate. The data are given in Table 1.

At relatively high rates of loading, the load versus time curves were straight lines; at lower rates, S-shaped curves were obtained. In the latter cases, the rates were derived from the straight portions of the curves.

4 TENSILE STRENGTH PROPERTIES OF ICE ADHERING TO STAINLESS STEEL

Table I. Tensile strength (kg/cm²) of snow-ice cylinders adhering to stainless steel, as a function of rate of stress application. Temp. = -4.5C; Vol. = 6.28 cm³; Area = 3.14 cm²; Height = 2 cm.

Stress Rate, (kg/cm ² -sec)	0.051	0.11	0.21	0.57	1.10
	14.6	12.2	17.2	15.5	17.8
	18.1	18.7	10.0	14.0	14.0
	16.0	15.5	14.7	13.2	14.3
	13.5	15.3	20.5	16.1	13.2
	15.3	18.6	18.9	13.4	17.6
	8.9	17.1	15.6	15.5	19.6
	13.2	19.9	20.4	15.3	16.2
	12.9	19.2	20.2	13.0	-
	17.4	14.7	20.3	19.1	-
	15.8	16.8	10.5	18.9	-
	17.1	19.5	19.0	13.5	-
	13.6	16.8	-	16.3	-
	-	13.0	-	19.1	-
Mean	14.7	16.7	17.0	15.6	16.1
Standard Deviation	± 2.6	± 2.5	± 3.9	± 2.2	± 2.1
Standard Error of Mean	± 0.7	± 0.7	± 1.2	± 0.6	± 0.8
Variance	6.8	6.3	15.3	4.9	4.4

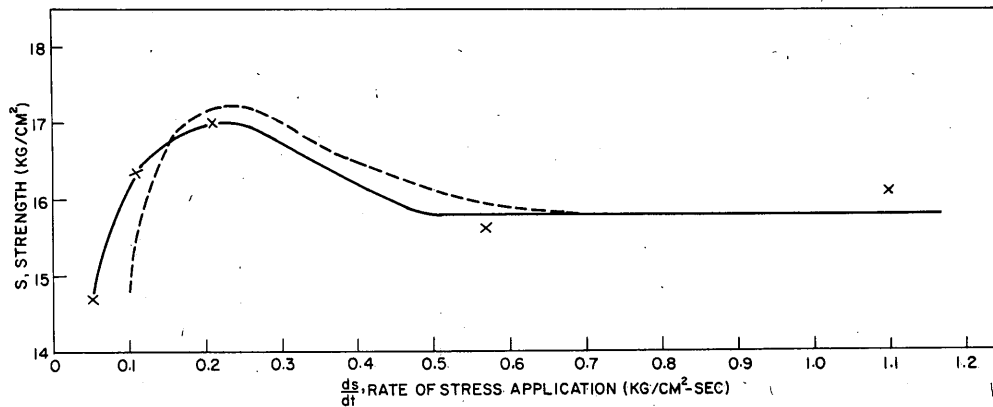


Figure 5. Average tensile strength as a function of rate of stress application for snow-ice cylinders (height 2 cm, diameter 2 cm). Dashed line is calculated curve according to equation (1).

Most of the breaks were partly cohesive and partly adhesive, usually exposing 20 to 30% of the metal surface (Fig.4A,B). In most cases, the breaks took place within 1-2 mm of one of the ice-metal interfaces and the rupture plane formed an angle of 10° to 20° with the metal surface. Occasionally the break was completely cohesive but still in the neighborhood of the interface and forming an angle with it (Fig. 4C). In a few instances, the rupture plane was at right angles to the cylinder axis, and, in very rare instances, such a rupture plane was situated near the middle of the cylinder (Fig. 4D). It was also observed that the breaks became more cohesive with increasing rates of loading. Figure 5 shows the tensile strength as a function of the rate of stress application for the snow-ice cylinders of 2 cm height and 2 cm diameter. It can be seen, that, as the rate of stress application increases, the tensile strength

values pass through a maximum and eventually reach a constant value indicating that they become independent of the rate of stress application. Similar curves were found by Komichevskaia (1951) for permafrost and ice. For our specimens, the tensile strength, S , as a function of rate of stress application, \dot{v} , can be expressed approximately by the equation:

$$S = C \left[\left(\frac{v\epsilon}{\epsilon v_m^{-1}} - 1 \right) e^{-\epsilon v} + 1 \right]; \text{ in this particular case, } \epsilon = 10 \text{ cm}^2\text{-sec/kg,} \quad (1)$$

$$v_m = 0.22 \text{ kg/cm}^2\text{-sec; and } C = 15.8 \text{ kg/cm}^2.$$

Tables II and III show the rate of loading and stress application as functions of the rate of the motor and height and area of the specimens. The rate values given in the tables are averages of all the respective strength measurements, which will be discussed in a subsequent section of this paper.

Table II. Rates of loading and stress application as a function of rpm of motor for snow-ice, at -4.5°C , (height = 2 cm, area = 3.14 cm^2).

Motor (rpm)	Rate of Loading (kg/sec)	Stress rate (kg/cm ² -sec)
15	0.16	0.051
30	0.35	0.11
60	0.66	0.21
179	1.79	0.57
355	3.46	1.10

Table III. Rates of loading and stress application as a function of area and height of the specimens, at -4.5°C ; speed of motor = 179 rpm.

Height (cm)	Area (cm ²)	Rate of loading (kg/sec)	Stress rate (kg/cm ² -sec)
2	3.14	1.93	0.61
1	3.14	2.07	0.66
0.076 to 0.127	1.54	1.94	1.26
0.025 to 0.152	0.782	1.92	0.46
0.025 to 0.127	0.332	1.64	4.95
0.025 to 0.127	0.196	1.35	6.90

It is seen that the rate of loading for a constant speed of the motor does not change appreciably with the area of the specimen. If all the strain were taken up by the ice, the strain rate should be constant for all specimens of equal height, irrespective of area. Hence, the rate of loading (kg/sec) should be proportional to the cross-sectional area and the rate of stress application should be constant. However, this is not the case. There is only a relatively small increase in loading rate with area. The height of the specimens has no marked effect on the rate of loading. This is due to the fact that most of the strain is taken up by the chains of the apparatus, as can be shown easily. Experiment No. 299, for example, was carried out at -4.5°C at a motor speed of 179 rpm; the duration of the test until rupture was 20 sec. The specimens were 0.127 cm high, and 1.54 cm^2 in area. As stated above, the vertical distance traveled by the rigid parts of the tensile strength apparatus was $3 \times 10^{-3} \text{ cm}$ for each revolution of the motor. For 60 revolutions, the distance traveled would be 0.18 cm, larger than the original thickness of the specimen. Hence, most of the strain is taken up by the chains.

Table IV shows some tensile strength values for different cross-sectional areas and equal heights at different rates of stress application. It is seen that the tensile

6 TENSILE STRENGTH PROPERTIES OF ICE ADHERING TO STAINLESS STEEL

strength values appear to be independent of stress rate, within the range employed. As all subsequent strength measurements were carried out in this range of areas and rates, the strength values can be considered to be independent of the rate of stress application.

Table IV. Tensile strength (kg/cm^2) for different cross-sectional areas and rates of stress application. Ice cylinders adhering to stainless steel. Temp. = -4.5°C .

Vol. = $1.17 \times 10^{-1} \text{ cm}^3$; area = 1.54 cm^2 Height = $7.62 \times 10^{-2} \text{ cm}$.			Vol. = $1.49 \times 10^{-2} \text{ cm}^3$; area = 0.196 cm^2 Height = $7.62 \times 10^{-2} \text{ cm}$.	
Rpm	355	89	355	89
Stress rate ($\text{kg}/\text{cm}^2\text{-sec}$)	2.81	0.82	13.8	3.22
	35.8	43.0	31.4	33.0
	32.7	27.1	34.6	33.0
	27.0	35.4	41.6	36.3
	41.0	35.0	27.1	30.1
	32.0	38.0	35.3	30.6
	42.0	36.3	40.8	34.6
	32.0	33.6	34.6	51.3
	40.9	27.8	41.8	26.5
	38.0	42.0	40.8	30.6
	40.2	42.2	32.0	26.5
	27.0	35.3	42.6	27.5
	34.7	27.5	41.6	32.6
Mean	35.3	35.3	37.0	32.7
Standard deviation	± 5.4	± 5.6	± 5.2	± 6.3
Standard Error of Mean	± 1.6	± 1.6	± 1.5	± 1.8
Variance	28.8	31.6	26.7	39.5

Tensile strength as a function of geometrical parameters

Tensile strength experiments were performed on thin disks prepared by freezing water in the manner described previously. In every instance, the breaks were completely cohesive, the rupture planes being situated nearer one of the metal ice interfaces for the thicker specimens. In some instances, the rupture surfaces appeared very smooth with only a small rough patch; in other instances, the whole rupture surface was rough. A typical rough surface is shown in Figure 6.

Many of the fractured disks were observed under polarized light. The grain size varied. Frequently there were one or two larger grains with a number of small ones. In other cases, the whole specimen consisted of relatively small grains. A preferred orientation was often observed, with the c -axis lying parallel to the cylinder axis.

Tables V-IX give the individual tensile strength data for ice specimens and snow-ice specimens. Figure 7 shows the average tensile strength values plotted as a function of the volume. Figure 8 shows the logarithms of the tensile strength plotted against the logarithms of the specimen volumes (snow-ice values not shown). The straight lines were obtained by the method of least squares. It is seen that the tensile strength increases very rapidly as the volume decreases. However, only values for any one area lie on a curve, each area forming a separate curve. The logarithms of the variances as a function of the log of the volumes are shown in Figure 9.



Figure 6. Typical rough surface of an ice film of original thickness 1.0×10^{-1} cm.

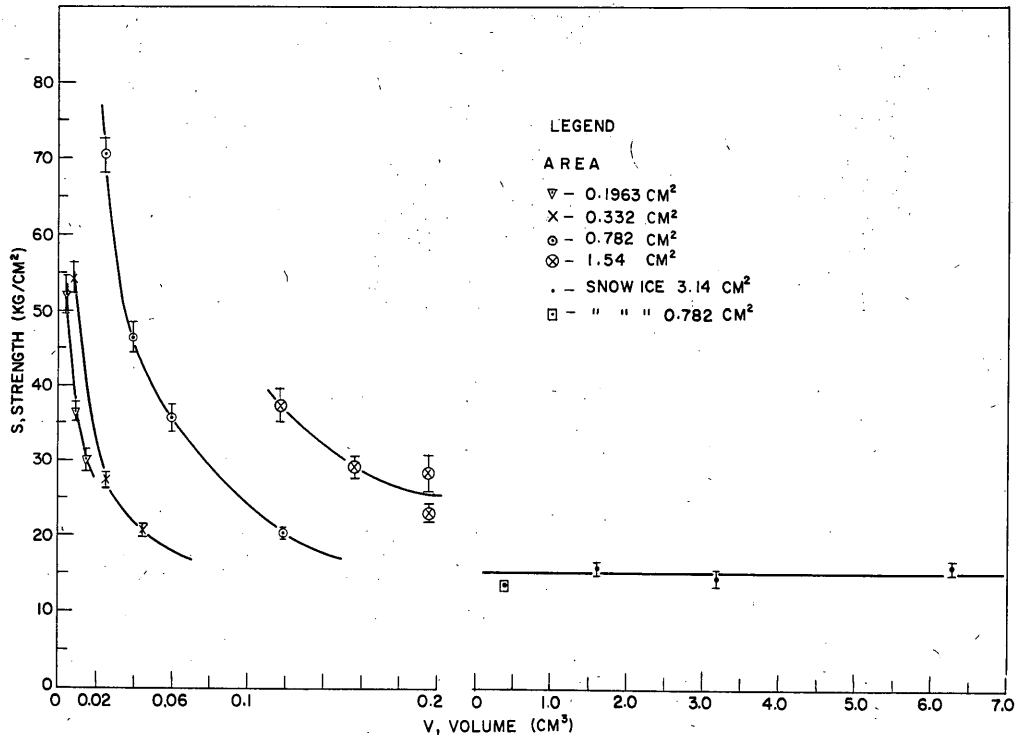


Figure 7. Average tensile strength as a function of ice volume (each point represents the average value of at least 12 tests). Ranges indicated are standard errors of the mean.

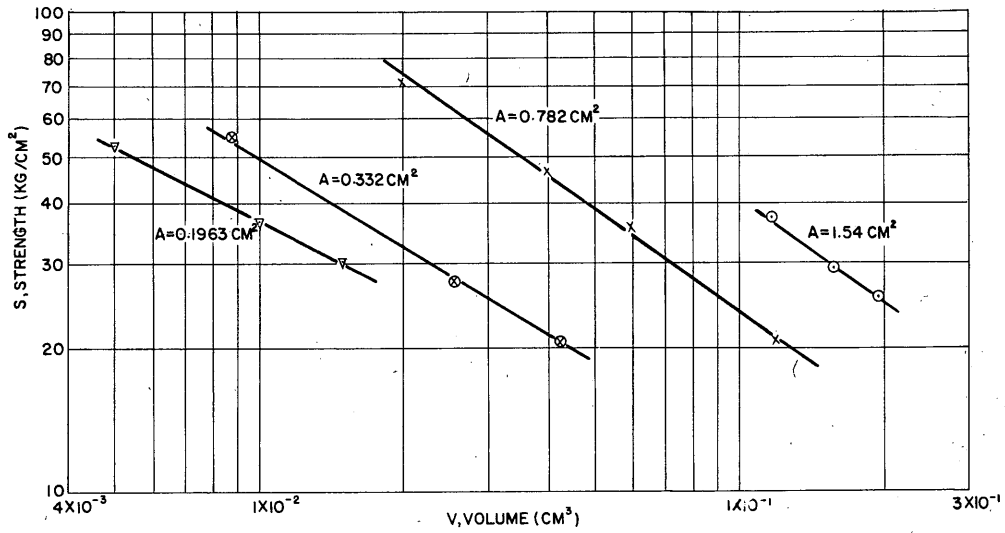


Figure 8. Logarithms of average tensile strengths as a function of logarithms of the volumes.

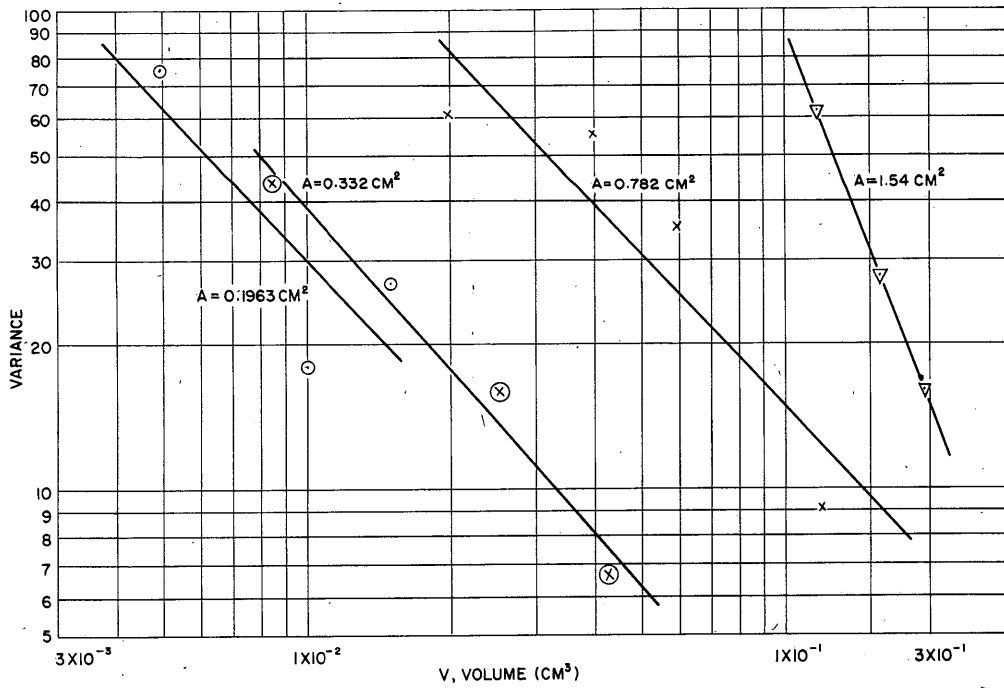


Figure 9. Logarithms of variances as a function of logarithms of volumes.

Table V. Tensile strength (kg/cm²) as a function of geometrical parameters, snow-ice cylinders adhering to stainless steel.Temp. = -4.5C; Stress rate = 0.64 kg/cm²-sec; Area = 3.14 cm².

Volume (cm ³)	1.57	3.14	6.28
Height (cm)	0.50	1.00	2.00
	18.9	13.4	15.5
	12.2	18.2	14.0
	15.3	11.7	13.2
	13.5	16.9	16.1
	16.3	15.3	13.4
	12.2	16.8	15.5
	11.0	12.0	15.3
	20.4	10.2	13.0
	16.3	14.3	19.1
	15.0	11.7	18.9
	17.8	-	13.5
	17.0	-	16.3
	-	-	19.1
	-	-	15.8
	-	-	11.2
	-	-	20.6
Mean	15.5	14.1	15.7
Standard deviation	± 2.9	± 2.7	± 2.7
Standard Error of Mean	± 0.8	± 0.9	± 0.7
Variance	8.3	7.2	7.0

Table VI. Tensile strength (kg/cm²) as a function of geometrical parameters, ice cylinders adhering to stainless steel.Temp. = -4.5C; Stress rate = 1.26 kg/cm²-sec; Area = 1.54 cm².

Volume (cm ³)	1.17 x 10 ⁻¹	1.57 x 10 ⁻¹	1.96 x 10 ⁻¹	1.96 x 10 ⁻¹
Height (cm)	7.62 x 10 ⁻²	1.02 x 10 ⁻¹	1.27 x 10 ⁻¹	1.27 x 10 ⁻¹
	38.0	32.2	25.9	22.5
	30.4	25.5	26.5	19.5
	35.3	27.8	24.6	24.8
	25.4	34.8	22.3	22.2
	38.9	33.2	28.0	22.2
	47.5	37.1	24.4	22.5
	39.0	30.9	25.2	19.1
	29.1	19.2	34.4	20.8
	41.5	26.2	42.6	21.2
	28.1	33.3	42.2	22.3
	46.7	23.4	35.5	22.9
	48.1	26.0	37.6	34.5
Mean	37.3	29.1	28.3	22.9
Standard deviation	± 7.9	± 5.6	± 8.1	± 4.0
Standard Error of Mean	± 2.3	± 1.5	± 2.3	± 1.2
Variance	61.6	27.9	65.7	15.9

10 TENSILE STRENGTH PROPERTIES OF ICE ADHERING TO STAINLESS STEEL

Table VII. Tensile strength (kg/cm²) as a function of geometrical parameters, ice cylinders adhering to stainless steel.

Temp. = -4.5C; Stress rate = 2.46 kg/cm²-sec; Area = 0.782 cm².

Volume (cm ³)	1.99 x 10 ⁻²	3.97 x 10 ⁻²	5.96 x 10 ⁻²	1.19 x 10 ⁻¹	0.391*
Height (cm)	2.54 x 10 ⁻²	5.08 x 10 ⁻²	7.62 x 10 ⁻²	1.52 x 10 ⁻¹	0.50
59.8	53.2	30.8	26.1	14.5	
58.2	42.0	41.0	20.5	11.0	
72.0	47.0	34.8	19.4	12.0	
59.4	54.2	41.0	25.6	18.2	
75.6	34.8	25.6	19.9	12.5	
75.7	33.8	43.0	23.0	16.2	
73.0	46.0	30.2	16.9	17.4	
72.6	47.1	35.8	19.0	12.8	
67.5	57.3	33.3	17.9	14.0	
81.5	49.0	44.1	20.0	10.1	
79.3	44.5	30.0	17.4	8.4	
70.0	-	40.1	22.5	14.1	
Mean	70.4	46.3	35.8	20.7	13.4
Standard deviation	± 7.8	± 7.4	± 6.0	± 3.0	± 2.9
Standard Error of Mean	± 2.2	± 2.1	± 1.8	± 0.9	± 0.8
Variance	60.2	55.1	35.5	9.1	8.4

* Snow-ice.

Table VIII. Tensile strength (kg/cm²) as a function of geometrical parameters, ice cylinders adhering to stainless steel.

Temp. = -4.5C; Stress rate = 4.95 kg/cm²-sec; Area = 0.332 cm².

Volume (cm ³)	8.43 x 10 ⁻³	2.53 x 10 ⁻²	4.24 x 10 ⁻²
Height (cm)	2.54 x 10 ⁻²	7.62 x 10 ⁻²	1.27 x 10 ⁻¹
47.0	27.3	21.4	
65.5	23.3	17.8	
51.6	24.8	19.3	
49.2	26.8	24.0	
64.1	30.5	20.1	
59.8	24.1	22.4	
58.3	31.1	26.0	
55.0	33.1	21.6	
55.7	33.7	18.8	
55.2	25.3	19.5	
51.6	29.8	17.8	
43.4	25.9	18.3	
Mean	54.7	27.5	20.6
Standard deviation	± 6.6	± 4.0	± 2.6
Standard Error of Mean	± 1.9	± 1.1	± 0.7
Variance	43.8	15.7	6.6

Table IX. Tensile strength (kg/cm²) as a function of geometrical parameters, ice cylinders adhering to stainless steel.Temp. = -4.5°C; Stress rate = 6.90 kg/cm²-sec; Area = 0.196 cm².

Volume (cm ³)	4.99 × 10 ⁻³	9.97 × 10 ⁻³	1.50 × 10 ⁻²
Height (cm)	2.54 × 10 ⁻²	5.08 × 10 ⁻²	7.62 × 10 ⁻²
	52.0	37.3	22.8
	60.0	37.9	32.0
	61.0	31.6	34.6
	57.0	33.0	36.7
	47.8	32.4	34.6
	52.0	40.7	35.7
	40.7	35.3	29.3
	56.0	41.8	30.6
	42.8	36.7	28.5
	59.0	44.8	20.8
	63.2	32.6	24.5
	36.6	33.4	29.5
Mean	52.3	36.5	30.0
Standard deviation	± 8.7	± 4.2	± 5.2
Standard Error of Mean	± 2.5	± 1.2	± 1.5
Variance	75.2	17.8	26.7

Figure 10 shows the tensile strength values plotted as a function of cross-sectional area at constant volume. Straight line relationships are obtained, which intersect the ordinate at finite values. The straight lines were again obtained by the method of least squares. The average value of these intercepts is $C = 9.4$ kg/cm². It appears that the tensile strength values obey an equation of the form:

$$S = kAV^{-b} + C. \quad (2)$$

Here, S is the tensile strength, A the cross-sectional area, V the volume, and k , b , and C are constants. Hence, by plotting the logarithms of $S - C/A$ against the logarithms of the volume V , a straight line should be obtained. That this is actually the case over an approximately thousandfold range of volumes is shown in Figure 11. The straight line was drawn by the method of least squares, not including the snow-ice values for 89 and 355 rpm. The corresponding equation is:

$$S = 2.74AV^{-0.84} + 9.4 \quad (3)$$

where S is in kg/cm², A in cm², and V in cm³.

Equation (2) can also be expressed in terms of the length or height of the specimens. Thus,

$$S = kA^{1-b}L^{-b} + C \quad (2a)$$

or

$$S = 2.74A^{0.16}L^{0.84} + 9.4. \quad (3a)$$

These equations will be of importance for the interpretation of the experimental data, as will become apparent in the discussion.

Temperature dependence

The average tensile strength data for ice films of height 7.62×10^{-2} cm and area 0.782 cm^2 as a function of temperature are shown in Table X. Measurements were carried out at -4.5 (see Table VII), -11 , -20 , -35 , and -45C . There is no appreciable dependence of tensile strength on temperature in this region, only a slight indication that the tensile strength will decrease rather than increase with decreasing temperatures. Butkovich (1954) found a slight increase of tensile strength with decreasing temperatures for commercial ice, which had rather large grains. Moreover, his specimens had cross-sectional areas of 3 cm^2 and were about 9 cm long with ends of larger cross-section. Thus, Butkovich's values are bulk tensile values, whereas the present ones are values for thin films constrained by stainless steel surfaces.

Table X. Tensile strength (kg/cm^2) as a function of temperature.
Ice cylinders adhering to stainless steel.
Height = 7.62×10^{-2} cm; Area = 0.782 cm^2 ; Volume = $5.96 \times 10^{-2} \text{ cm}^3$.

Temperature (C)	-11	-20	-35	-45
Rate of stress application ($\text{kg}/\text{cm}^2\text{-sec}$)	2.7	2.8	2.7	2.3
	35.6	33.4	31.7	30.2
	28.0	38.2	39.5	33.1
	32.7	54.2	51.2	22.0
	43.0	30.1	37.3	25.0
	31.0	30.0	36.0	42.0
	35.0	37.0	36.4	25.1
	35.5	33.0	25.8	24.0
	32.0	43.3	21.5	20.1
	28.6	30.0	31.7	18.2
	36.3	41.0	27.3	28.2
	23.5	37.1	29.0	17.0
	24.6	58.0	48.5	26.0
Mean	32.2	38.8	34.7	25.9
Standard deviation	± 5.5	± 9.2	± 8.7	± 6.9
Standard Error of Mean	± 1.6	± 2.7	± 2.5	± 2.0
Variance	30.3	84.5	75.3	47.9

DISCUSSION

Tensile strength as a function of rate of loading for snow ice.

The data are shown in Table I and Figure 5. The ruptures always took place in the neighborhood of one of the metal snow-ice interfaces. This indicates that there is a certain stress concentration near the interface, which is undoubtedly due to the constraint exerted on the ice by the adherence of the ice to the metal plate. A relevant discussion of this point by Alstadt is to be found at the end of a paper on the strength behavior of adhesive bonds by Meissner and Baldauf (1951). During load application on snow-ice, not only elastic deformation but also plastic flow takes place, as was clearly shown in a previous paper (Jellinek and Brill, 1956). This deformation and flow cause an additional stress concentration lateral to the interface. This is somewhat counteracted by stress relaxation, which always takes place during plastic flow. Thus, rupture takes place preferably in the vicinity of the interface. The fact that the break is partly cohesive and to a smaller extent adhesive is accounted for as follows:

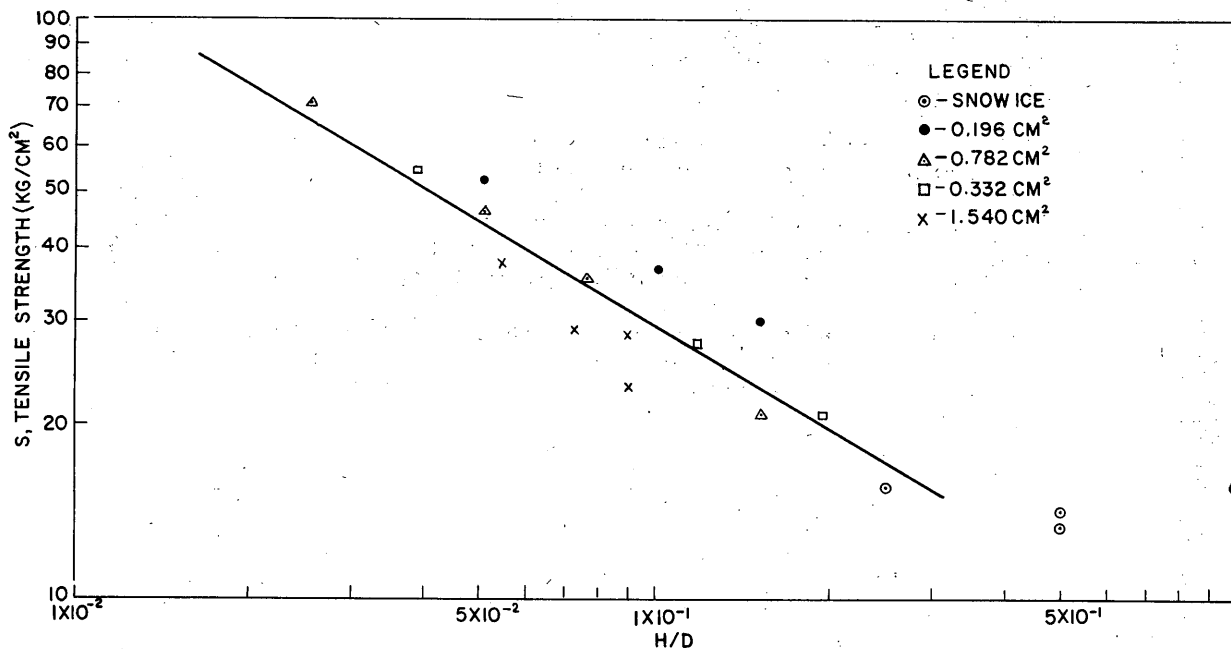


Figure 12. Logarithms of tensile strengths as a function of the logarithms of the ratio H/D of height to diameter of the ice cylinder.

The break starts in the ice near the interface and at an angle of 10 to 20 degrees towards it. Thus, in most cases, the rupture has to reach the interface before it is completed. By the time the rupture has reached the interface, tensile stress and an added torque are active at the interface. Such a torque produces a peeling action. It is well known that adhesive bonds succumb relatively easily to a peeling action. It is almost certain that the rupture is not initiated at the interface, as the adhesional strength of ice to stainless steel is very much larger than the cohesive strength of ice. This will become clear during the subsequent discussion of the rupture of thin ice disks.

The change of tensile strength with the rate of loading can now be explained as follows: At low speeds of loading, an appreciable plastic flow takes place, which is apparent from the non-linearity of the recorded load versus time curves. Hence, an appreciable lateral stress component will be present in the neighborhood of the interface, and, though counteracted by a certain amount of stress relaxation, will lead to smaller tensile strength values. At high speeds of loading, less plastic flow will take place and the lateral stress component will decrease. Therefore, the tensile strength should be higher than at relatively low rates of loading. However, at the high rates, stress relaxation will be small, which in turn will tend to decrease the tensile strength. Hence, there will be an optimum region of loading rates where all these effects will combine to give a maximum tensile strength, which is actually observed.

As pointed out previously, the rupture of thin ice disks shows characteristics different from those of larger samples. The break is always completely cohesive and the tensile strength is a function of the volume, thickness, and diameter of the cylinders.

Tensile strength of ice cylinders as a function of geometrical parameters

First, the discussion may be based on the distribution of stresses, as was proposed, for instance, by Meissner and Baldauf (1951). They point out that a quantitative, mathematical analysis of stress distribution in a cylinder has not yet been carried out, but that there should be a general correlation between tensile strength and the ratio of height to diameter of the cylinder. They further state, without giving substantial reasons, that the strength should increase with decreasing

length or height of the specimens. Berghausen *et al.* (1953) set up general equations for stress distributions in a cylinder, but did not solve them. Figure 12 shows an approximate straight-line relationship between the logarithms of the tensile strength and the logarithms of the ratio of height to diameter of the specimens. However the points for each area are still clearly discernible as belonging together. The equation for the logarithmic straight line obtained by the method of least squares (excluding the snow-ice values) is:

$$S = 7.6[H/D]^{-0.59} \text{ kg/cm}^2.$$

In spite of this approximate correlation between the tensile strength and the ratio of height to diameter, the above assumption that the change in tensile strength with geometrical parameters is due to stress distribution is untenable.

It is well known that all crystalline substances have imperfections (e. g. dislocations). Such imperfections explain the large discrepancies between tensile strength values deduced from theoretical considerations and those found by experiment. An approximate theoretical strength value for ice can be deduced quite easily from the equation

$$S = \frac{2\gamma}{d}$$

where S is the strength, γ the free surface energy for unit area, and d the distance over which the work of rupture has to take place. For $\gamma_{\text{H}_2\text{O}} = 76 \text{ erg/cm}^2$ and $d = 2 \times 10^{-8} \text{ cm}$, one obtains a conservative estimate of $S = 7600 \text{ kg/cm}^2$. The bulk tensile strength of ice found by experiment is only about 15 kg/cm^2 . Thus, it is clear that imperfections will have to be considered in any theory concerning tensile strength.

It will be assumed here that there is a definable distribution of imperfections in the ice. This distribution is considered in relation to the strength of the imperfections. This means that each imperfection can withstand stresses up to a certain critical value. When this critical stress is reached, the imperfection opens up to a crack and the specimen is ruptured. The spatial distribution of the imperfections is assumed to be random and the number of imperfections proportional to the specimen volume. In large specimens, the whole distribution of imperfections will be represented from the weakest to the strongest. In small specimens, not all types of imperfections will be present; those in the neighborhood of the distribution maximum will be predominant. The relevant statistics are briefly presented here.

The underlying distribution of imperfections of different strengths is given by $y = f(S)$, where y is the frequency of imperfections of strength S . As soon as the stress S is reached, the imperfection opens up and produces rupture of the specimen. The strength of each specimen will be given by its weakest imperfection. The problem is to calculate the frequency distribution for these weakest imperfections, or the distribution of tensile strengths for the specimens. Such a distribution can be obtained experimentally from a large number of tensile-strength experiments.

Specimens of volumes which have r imperfections each will be considered now. The probability of obtaining a specimen whose weakest imperfection corresponds to a tensile strength S is given by:

$$P_r = r f(S) dS \left[\int_S^\infty f(S) dS \right]^{r-1}; \quad (4)$$

$f(S) dS$ is the probability of having an imperfection of strength between S and $S+dS$ in the sample

$$\left[\int_0^\infty f(S) dS = 1 \right];$$

$$\left[\int_S^{\infty} f(S) dS \right]^{r-1}$$

gives the probability that all other imperfections are of strength larger than \underline{S} , \underline{r} gives the number of ways in which this particular assembly of imperfections can be achieved. Equation (4) can also be expressed by means of the cumulative or integral distribution of $f(S)$ since

$$\int_0^S f(S) dS = F(S),$$

where $F(S)$ is the cumulative distribution. Hence:

$$P_r = r f(S) dS [1-F(S)]^{r-1} \quad (5)$$

$$f_r(S) = r f(S) [1-F(S)]^{r-1} \quad (5a)$$

The cumulative distribution for specimens containing \underline{r} imperfections is obtained by integrating equation (5a) and the most probable value by finding the maximum for equation 5a, hence:

$$\int_0^S f_r(S) dS = F_r(S) = 1 - [1-F(S)]^r \quad (6)$$

$$(r-1) f^2(S_{\max}) = f'(S_{\max}) [1-F(S_{\max})] \quad (7)$$

The average tensile strength of the specimens is given by:

$$\bar{S}_r = \int_0^{\infty} S f_r(S) dS \quad (8)$$

The variance given by the square of the standard deviation σ is:

$$\sigma^2 = \int_0^{\infty} f_r(S) [S - \bar{S}_r]^2 dS \quad (9)$$

According to the assumptions outlined above, $r = kV$, where \underline{k} is a constant and \underline{V} the volume of the specimen containing \underline{r} imperfections.

It remains now to introduce for $f(S)$ a specific distribution. Weibull (1939) introduced a distribution function, which seems to represent experimental data quite satisfactorily in many cases. The relevant equations are collected in Table XI below, which shows that the average strength value of the samples should only depend on the volume and should be proportional to $\underline{V}^{-1/\beta}$, and that the variance should be proportional to $\underline{V}^{-2/\beta}$ where β is a constant.

The experimental average tensile strength values are proportional to $\underline{V}^{-1/\beta}$ (Fig. 8). However, a separate curve is obtained for each cross-sectional area, the strength values increasing linearly with the areas at constant volumes. The equations for the straight lines shown in Figure 8 (179 rpm values only) and the equations for the corresponding variances (Fig. 9), both obtained by the method of least squares, are as follows:

Area (cm ²)	Height (cm)	Tensile strength (kg/cm ²)	Variance
1.54	0.762 to 1.27 x 10 ⁻¹	$\bar{S} = 5.46 \underline{V}^{-0.92}$	$\sigma^2 = 0.22 \underline{V}^{-2.6}$
0.782	0.254 to 1.52 x 10 ⁻¹	$\bar{S} = 4.79 \underline{V}^{-0.70}$	$\sigma^2 = 1.3 \underline{V}^{-1.1}$
0.332	0.254 to 1.27 x 10 ⁻¹	$\bar{S} = 3.04 \underline{V}^{-0.61}$	$\sigma^2 = 0.1 \underline{V}^{-1.14}$
0.196	0.254 to 0.762 x 10 ⁻¹	$\bar{S} = 3.49 \underline{V}^{-0.51}$	$\sigma^2 = 0.22 \underline{V}^{-1.1}$

Table XI. Equations based on Weibull's (1939) distribution function.
 a and β are constants.

Underlying distribution function: $f(S) = a\beta S^{\beta-1} e^{-aS^\beta}$

Cumulative distribution: $F(S) = 1 - e^{-aS^\beta}$

Distribution of weakest imperfections
 in volumes having r imperfections: $f_r(S) = ra\beta S^{\beta-1} e^{-raS^\beta}$

Introducing $r = kV$: $f_r(S) = kVa\beta S^{\beta-1} e^{-kVaS^\beta}$

Cumulative distribution: $F_r(S) = 1 - e^{-raS^\beta}$

Most probable value: $r S_{\max}^3 + S_{\max}^\beta = \frac{\beta-1}{a\beta}$

Average strength value: $\bar{S}_r = \frac{\Gamma(1/\beta+1)}{(ra)^{1/\beta}} = \frac{\Gamma(1/\beta+1)}{(kVa)^{1/\beta}}$

Variance: $\sigma^2 = \frac{\text{const.}}{(kaV)^{2/\beta}}$

As can be seen from these data, the exponents for the volumes in the expressions for the variances are about twice those in the strength equations. Thus, on the whole, the data fit the statistical theory, except for the marked influence of the cross-sectional area. Berghausen et al. (1953) found that their data gave approximately a straight line when the tensile strengths were plotted against the logarithms of the volumes.

They concluded that the dependence of the strength on the volume is due to a statistical effect involving imperfections. However, they did not attempt a detailed analysis. Their standard deviations are at least two to four times larger than those obtained in this work and the influence of the cross-sectional areas is rather obscured owing to the large scatter of the experimental values.

It is clear that the dependence of the tensile strength on the specimen volume is due to a statistical effect, most reasonably explained by imperfections. However, the statistical treatment as outlined above only accounts for certain aspects of the experimental data.

An attempt will now be made to account for the influence of the area on a statistical basis. For this purpose, the assumption that the whole specimen ruptures as soon as the strength of the weakest imperfection is reached will be modified. It will be assumed now that, when the strength of an imperfection is reached, a crack is formed which does not grow beyond a certain unspecified average size. Thus, there will be stress relief in the neighborhood of this crack and the next stronger imperfection will open up; the specimen will rupture when a string of cracks has formed in cascade fashion across the specimen. It is very difficult to treat such a model mathematically on a statistical basis. A simpler problem, which constitutes an approximation to the above model, is treated here. The specimen is considered as a bundle of parallel rods of equal cross-section and length. An imperfection which opens into a crack only "ruptures" the rod in which it is situated. Thus, the problem

18 TENSILE STRENGTH PROPERTIES OF ICE ADHERING TO STAINLESS STEEL

reverts to the case of the strength of a bundle of parallel threads encountered with textiles. This problem has been developed to a certain extent by Weibull (1939) However, as pointed out by Daniels (1945), his probabilities were not chosen correctly. Daniels has elaborated the statistics of such parallel systems, but operated only with cumulative distributions and studied the behavior of such distributions and their average values for large numbers of parallel elements. The statistics is developed here starting with derivative distributions, which allow average values to be calculated.

In the case of one rod having a volume which contains \underline{r} imperfections, the breaking load-frequency distribution is given by equation (5a). Loads are used here in preference to stress. Hence, the probability of having such a rod of breaking load \underline{L} is given by:

$$P_r = r f(L) dL [1 - F(L)]^r \quad (\text{when } \underline{r} \text{ is large})$$

The condition for \underline{n} parallel rods to break under exactly a load \underline{L} , in terms of L , is given below:

Rod	Case						
	1	2	3	4	...	n-1	n
1	1	$1 \rightarrow \frac{1}{2}$	$1 \rightarrow \frac{1}{3}$	$1 \rightarrow \frac{1}{4}$...	$1 \rightarrow \frac{1}{n-1}$	$1 \rightarrow \frac{1}{n}$
2	$\frac{1}{2} \rightarrow 0$	$\frac{1}{2}$	$\frac{1}{2} \rightarrow \frac{1}{3}$	$\frac{1}{2} \rightarrow \frac{1}{4}$...	$\frac{1}{2} \rightarrow \frac{1}{n-1}$	$\frac{1}{2} \rightarrow \frac{1}{n}$
3	$\frac{1}{3} \rightarrow 0$	$\frac{1}{3} \rightarrow 0$	$\frac{1}{3}$	$\frac{1}{3} \rightarrow \frac{1}{4}$...	$\frac{1}{3} \rightarrow \frac{1}{n-1}$	$\frac{1}{3} \rightarrow \frac{1}{n}$
4	$\frac{1}{4} \rightarrow 0$	$\frac{1}{4} \rightarrow 0$	$\frac{1}{4} \rightarrow 0$	$\frac{1}{4}$...	$\frac{1}{4} \rightarrow \frac{1}{n-1}$	$\frac{1}{4} \rightarrow \frac{1}{n}$
.
.
n-2	$\frac{1}{n-2} \rightarrow 0$	$\frac{1}{n-2} \rightarrow 0$	$\frac{1}{n-2} \rightarrow 0$	$\frac{1}{n-2} \rightarrow 0$...	$\frac{1}{n-2} \rightarrow \frac{1}{n-1}$	$\frac{1}{n-2} \rightarrow \frac{1}{n}$
n-1	$\frac{1}{n-1} \rightarrow 0$	$\frac{1}{n-1} \rightarrow 0$	$\frac{1}{n-1} \rightarrow 0$	$\frac{1}{n-1} \rightarrow 0$...	$\frac{1}{n-1}$	$\frac{1}{n-1} \rightarrow \frac{1}{n}$
n	$\frac{1}{n} \rightarrow 0$	$\frac{1}{n} \rightarrow 0$	$\frac{1}{n} \rightarrow 0$	$\frac{1}{n} \rightarrow 0$...	$\frac{1}{n} \rightarrow 0$	$\frac{1}{n}$

The equation of the frequency distribution for \underline{n} parallel rods is given by an expression as follows:

$$f_{r,n}(L) = n! f_r(L) \prod_{a=1/n}^{1/2} \int_0^{aL} f_r(L) dL +$$

$$\begin{aligned}
 & + n! f_r\left(\frac{1}{2}L\right) \int_{\frac{1}{2}L}^{1L} f_r(L) dL \prod_{a=1/n}^{1/3} \int_0^{aL} f_r(L) dL + \\
 & + n! f_r\left(\frac{1}{3}L\right) \int_{\frac{1}{3}L}^{\frac{1}{2}L} f_r(L) dL \int_{\frac{1}{3}L}^{1L} f_r(L) dL \prod_{a=1/n}^{1/4} \int_0^{aL} f_r(L) dL + \\
 & + n! f_r\left(\frac{1}{4}L\right) \int_{\frac{1}{4}L}^{\frac{1}{3}L} f_r(L) dL \int_{\frac{1}{4}L}^{\frac{1}{2}L} f_r(L) dL \int_{\frac{1}{4}L}^{1L} f_r(L) dL \prod_{a=1/n}^{1/5} \int_0^{aL} f_r(L) dL + \dots \\
 & + n! f_r\left(\frac{1}{n}L\right) \left[\int_{\frac{1}{n}L}^{\frac{1}{n-1}L} f_r(L) dL \int_{\frac{1}{n}L}^{\frac{1}{n-2}L} f_r(L) dL \dots \int_{\frac{1}{n}L}^{1L} f_r(L) dL \right]. \tag{10}
 \end{aligned}$$

The average breaking load in the case of the Weibull distribution is given by expressions as follows (two rods):

$$\bar{L}_{r,2} = \frac{\Gamma(1/\beta+1)}{(ra)^{1/\beta}} 2! \left\{ 1 - \left[1 + \left(\frac{1}{2}\right)^\beta \right]^{-(1+1/\beta)} \left[1 + \left(\frac{1}{2}\right)^\beta - 1 \right] + 2^{\beta-1/\beta} \right\}$$

$$\text{or } \bar{L}_{r,2} = \frac{\Gamma(1/\beta+1)}{(ra)^{1/\beta}} 2! C_2 \tag{11}$$

where C_2 is a constant. The average tensile strength is given by:

$$\bar{S}_{r,2} = \frac{\Gamma(1/\beta+1)}{(ra)^{1/\beta}} \frac{2! C_2}{2A_1} \tag{12}$$

where A_1 is the cross sectional area of a single rod. The average value for three rods is given by,

$$\bar{L}_{r,3} = \frac{\Gamma(1/\beta+1)}{(ra)^{1/\beta}} 3! C_3.$$

The values for the constants C_1 , C_2 , C_3 and C_4 have been calculated for $\beta=1$ and $\beta=2$ and are given below:

	C_1	C_2	C_3	C_4
$\beta = 1$	1.00	1.10	0.79	0.45
$\beta = 2$	1.00	1.34	1.01	0.63

It can be seen that the theoretical stress values for constant heights of the specimen rise rather steeply if the number of parallel rods is small. Figure 13 shows the experimental tensile strength values plotted against the cross-sectional areas of the specimens at constant heights; for height values between about 6×10^{-2} to 2×10^{-1} cm, the strength values do not change appreciably with area. However, for smaller heights this increase becomes more appreciable. The observed increases are not large enough to justify the assumption of a small number of parallel elements.

Daniels (1945) has shown that, as the number of parallel rods, n , becomes very large; the average breaking load is approximately given by:

$$\bar{L}_{r,n} = n \times \text{constant.} \quad (13)$$

At the same time, the strength-frequency distribution approximates a normal distribution. Equation (13) holds if $1 - F_r(L)$ tends to zero faster than $1/L$. This is the case for the Weibull distribution as

$$e^{-raL^\beta} \quad (\text{for } \beta \geq 1)$$

tends to zero faster than $1/L$. Hence, for large values of n , one obtains,

$$\bar{L}_{r,n} = \frac{\Gamma(1/\beta+1)}{(ra)^{1/\beta}} n! C_n$$

or

$$\bar{L}_{r,n} = \frac{\Gamma(1/\beta+1)}{(ra)^{1/\beta}} nc \quad (14)$$

where c is a constant. The average tensile strength is then given by:

$$\bar{S}_{r,n} = \frac{\Gamma(1/\beta+1) C}{(ra)^{1/\beta} A_1}; \quad (15)$$

r in this case is proportional to the length of the sample $r = kL$, hence equation (15) can be written as,

$$\bar{S}_{r,n} = kL^{-1/\beta}$$

A few words may be added about the meaning of the constants in equation (15); r, β and with it c are dimensionless numbers; a has the dimensions of $(\text{kg})^{-\beta}$ and A that of cm^2 ; a is also given by

$$a = \left[\frac{\Gamma(1/\beta+1)}{\bar{L}} \right]^\beta$$

where \bar{L} is the average breaking load of a specimen of ice containing one imperfection, or in other words, \bar{L} is the average of the underlying Weibull distribution.

It was shown by Weibull that if the underlying distribution starts at a finite value a constant C has to be added to the equation. Hence, the final equation reads:

$$S_{r,n} = kL^{-1/\beta} + C. \quad (16)$$

Equation (16) becomes identical with the empirical equation (2a) for

$$b = 1/\beta = 1.$$

The present values show that $b = 0.84$. Equation (16) can also be written in the form:

$$\bar{S}_{r,n} = kA^{1/\beta}V^{-1/\beta} + C. \quad (17)$$

Thus, it appears that the statistical treatment accounts well for the experimental results except for a relatively small residual area effect. Equation (17) becomes identical with the empirical equation (2):

$$S = kAV^{-b} + C,$$

if the exponent for A becomes unity; actually, the exponent $1/\beta = b = 0.84$. The variance, following Daniels (1945), can be written as follows;*

$$\sigma^2 = \frac{1}{(\alpha\beta)^{2/\beta}} (e^{-1/\beta} - e^{-2/\beta})$$

or

$$\sigma^2 = \frac{A^{2/\beta}}{(\alpha\beta V)^{2/\beta}} (e^{-1/\beta} - e^{-2/\beta}).$$

As was seen previously, the variances go approximately proportional to $V^{-2/\beta}$.

Though the statistical result represents the experimental data quite well, there is still a noticeable cross-sectional area effect. This is believed to be due to two causes. First, the statistical model is only an approximate one, and second, there is probably a stress distribution effect superimposed on the statistical effect.

As was previously pointed out, the large ice cylinders break predominantly in the neighborhood of the metal ice interface, usually in a region of 1 to 2 mm from the interface. This is caused by the combined effect of stress distribution and imperfections. The location of the rupture is due to the stress concentration in the neighborhood of the interfaces. The magnitude, however, of the tensile strength is largely conditioned by the imperfections. Only occasionally, an especially weak imperfection is present outside the interfacial zones, which ruptures before a weak imperfection opens up near the interface. This situation will prevail until the specimens are decreased to a thickness where the stress concentration regions overlap. Then the statistical aspect will become predominant, as is actually the case. The stress distribution effect still makes itself felt in the residual observed influence of the cross-sectional area.

* Daniels' $b(s)$ is $F_r(S)$ here.

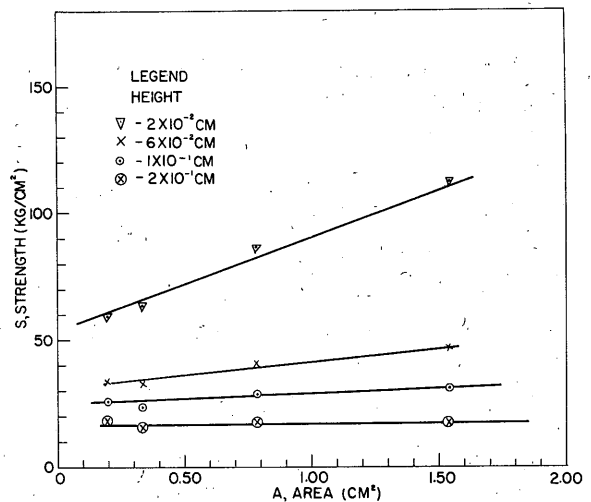


Figure 13. Tensile strength as a function of cross-sectional area at constant height.

REFERENCES

- Applied Science Research Laboratory, University of Cincinnati (1950-52). Investigation of the chemical-physical nature of adhesion of ice to solid surfaces, Progress Reports No. 1-8.
- _____ (1952-54) A study of the physical chemical nature of adhesion of ice to solid surfaces, Reports No. 1, 2, 4-8.
- Berghausen, P. E.; Good, R. J.; Kraus, G.; Podolsky, B.; and Soller, W. (1953) A study of chemical-physical nature of adhesion of ice to solid surfaces, University of Cincinnati, WADC Tech. Report 53-461.
- _____ et al. (1955) Fundamental studies of the adhesion of ice to solids, WADC Tech. Report 55-44.
- Butkovich, T. R., (1954) Ultimate strength of ice, Snow Ice and Permafrost Research Establishment, Corps of Engineers, U. S. Army, Research Paper 11.
- Daniels, H. E., (1945) Statistical theory of the strength of bundles of threads, I., Proceedings of the Royal Society (London), vol. 183, p. 405.
- DeBruyne, N. A., Editor (1951) Adhesion and adhesives, Elsevier Publishing Company.
- Epstein, B. (1948) Statistical aspects of fracture problems, Journal of Applied Physics, vol. 19, p. 140.
- Jellinek, H. H. G., and Brill, R. (1956) Viscoelastic properties of ice, Journal of Applied Physics, vol. 27, no. 10, p. 1198-1209.
- Khomichevskaja, L. S. (1940) O vremennom soprotivlenii szhatiiu vechnomerzlykh gruntov i l'da estestvennoi structure (The compressive strength of permafrost and ice in their natural states), Trudy Komiteta po vechnoi merzlobe, vol. X, p. 37-83, Translated by St. Anthony Falls Hydraulic Laboratory, University of Minnesota. for St. Paul District, Corps of Engineers. Project Report no. 26, October 1951.
- Meissner, H. P., and Baldauf, G. H. (1951) Strength behavior of adhesive bonds, Transactions, American Society of Mechanical Engineers, p. 697.
- Peirce, F. T. (1926) Tensile tests for cotton yarns, part V. The weakest link. Theorems on the strength of long and of composite specimens, Journal, Textile Institute. vol. 17, p. 355.
- Weibull, W. (1939a) A statistical theory of the strength of materials, Ing. Vetenskaps Akad. Handl. No. 151.
- _____ (1939b) The phenomenon of rupture in solids, Ing. Vetenskaps Akad. Handl. No. 153.